In Situ Measurement of Cation Order and Domain Growth in an Electroceramic

S. M. Moussa,[†] R. M. Ibberson,*[,‡] M. Bieringer,[§,||] A. N. Fitch,[⊥] and M. J. Rosseinsky*[,†]

Department of Chemistry, The University of Liverpool, Liverpool L69 7ZD, U.K., ISIS Facility, CLRC Rutherford Appleton Laboratory, Chilton, Didcot, Oxon, OX11 0QX, U.K., Institut Laue-Langevin, 6 rue Jules Horowitz, BP 156, F- 38042 Grenoble Cedex, France, and European Synchrotron Radiation Facility, BP 220, F-38043 Grenoble Cedex, France

Received December 9, 2002. Revised Manuscript Received March 18, 2003

In situ methods are ideally suited for the study of the development of property-critical structural features during materials processing. As an example of their potential in the area of complex oxide electroceramics, here, we apply in situ synchrotron powder diffraction to investigate the ordering processes responsible for optimizing the microwave dielectric properties of the commercial electroceramic barium zinc tantalate. The collection of synchrotron diffraction data with high resolution and high intensity during processing has allowed the growth of cation site order within a domain and the size of the ordered domains to be separated during the multistage thermal treatment processing used by industry. Domain growth does not commence until the extent of order within a domain is maximized. Analysis of the superstructure intensities with the Avrami equation shows that nucleation is not important in this process. Domain growth then occurs by the curvature-driven Allen−Cahn mechanism. The complex nature of the ordering is confirmed by the coexistence of two phases whose temporal evolution divides into two stages according to the two stages of ordering and domain growth mentioned above. The implications of these observations for industrial processing procedures aimed at reducing the processing time are discussed.

Introduction

Ordering processes in solids occur with symmetry lowering that leads to the formation of antiphase domains when the ordering occurs on different sublattices or of orientational domains when it occurs in different spatial directions.[1] Much of modern electroceramic processing is aimed at the control of the magnitude of the order parameters (which quantify the extent of order) within the domains and the spatial extent of the domains.[2] The extent of the order, the size of the ordered domains, and the energies of the associated domain boundaries can have a dramatic effect on the required physical property. An important example of this is the barium zinc tantalate ($Ba_3ZnTa_2O_9$, BZT) family of microwave dielectric resonators.[3,4] The initial processing affords a material with the Zn^{2+} and Ta^{5+} cations largely disordered over the octahedral B site of the ABO_3 perovskite structure. This material, despite its high dielectric constant, has large dielectric losses at microwave frequencies and thus a low value of $Q = (\tan \delta)^{-1}$, making it unsuitable for its target application in cellular telephone base stations. A second processing step is required to afford both resonator densification and the growth of domains of a trigonal cation ordered structure in which one layer of ZnO_6 octahedra alternates with bilayers of TaO_6 octahedra along one of the ⟨111⟩ directions of the perovskite unit cell, which becomes the *c* axis in the trigonal structure (Figure 1). This strict layered site ordering of the Zn and Ta cations is required to minimize the dielectric loss at microwave frequencies (i.e., to maximize *Q*) and presumably involves ordering of Zn and Ta atoms over the B sites by jump interchange of these species. Selection of the four possible layer ordering directions results in the formation of orientational domains, while faulting in the strict mono/bilayer cation alternation gives rise to translational or antiphase domains.[5] These ordered phases have ideal properties for microwave dielectric resonators in mobile telecommunications base stations but require careful processing. Commercial applications require shortening of the processing time to optimal performance, which is achieved by the addition of dopants such as Zr[6] and Ga[7] on the B site, associated with minimizing the effect of domain wall strains on the

* Authors to whom correspondence should be addressed. E-mail: m.j.rosseinsky@liv.ac.uk (M.J. Rosseinsky); r.m.ibberson@rl.ac.uk (R.M. Ibberson).
[†] The University of Liverpool.
[‡] Rutherford Appleton Laboratory
[§] Institut Laue-Langevin
[||] Present address: University of Manitoba, Department of Chemistry, 506 Parker Building, Winnipeg, Manitoba, R3T 2N2 Canada.
[⊥] European Synchrotron Radiation Facility.

(1) Kozubski, R. *Prog. Mater. Sci.* **1997**, *41*, 1−59.
(2) Davies, P. K. *Curr. Opin. Solid State Mater. Sci.* **1999**, *4*, 467−471.
(3) Tamura, H.; Konoike, T.; Sakabe, Y.; Wakino, K. *J. Am. Ceram. Soc.* **1984**, *67*, C59−C61.
(4) Desu, S.; O'Bryan, H. M. *J. Am. Ceram. Soc.* **1985**, *68*, 546−551.
(5) Reaney, I. M.; Colla, E. L.; Setter, N. *Jpn. J. Appl. Phys.* **1994**, *33*, 3984−3990.
(6) Davies, P. K.; Tong, J. Z.; Negas, T. *J. Am. Ceram. Soc.* **1997**, *80*, 1727−1740.
(7) Kageyama, K. *J. Am. Ceram. Soc.* **1992**, *75*, 1767−1771.

10.1021/cm020476c CCC: $25.00
Published on Web 05/28/2003

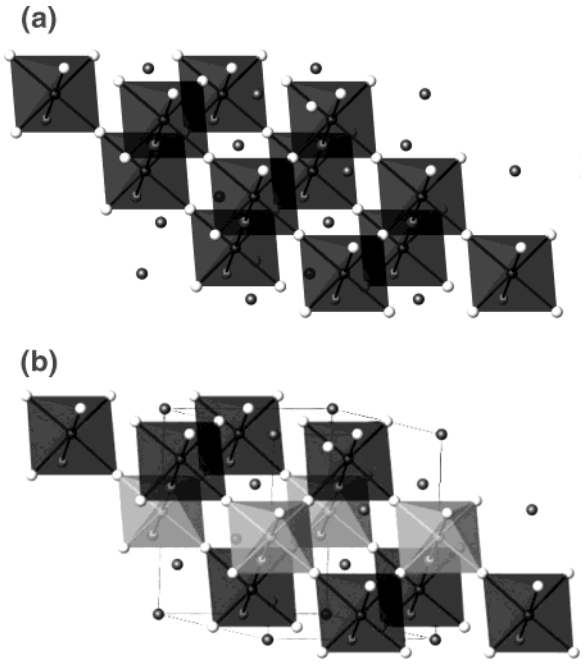

Figure 1. Structure of $Ba_3ZnTa_2O_9$: (a) cubic B-site-disordered perovskite that represents the material in its calcined state before the annealing procedure studied in situ by X-ray powder diffraction, (b) trigonal B-site-ordered perovskite with alternate layers of TaO_6 (dark shading) and ZnO_6 (light shading) octahedra that is the idealized 2:1 ordered structure of BZT. In both figures, the [111] direction of the cubic perovskite subcell is vertical, corresponding to the trigonal *c* axis.

dielectric loss. This annealing step is hard to control because of the competition between the rate of ordering and the thermodynamic extent of ordering, which are affected in opposite ways by increasing temperature, coupled with the problem of the loss of volatile ZnO.

Current understanding of the required materials processing is due in large part to empirical trial-and-error studies and ex situ characterization techniques. In situ methods offer the opportunity to study how property-critical parameters evolve in real time during processing and can identify key points where these parameters develop in a nonmonotonic manner, corresponding to critical points in the materials processing. In this paper, we use in situ synchrotron X-ray powder diffraction at high temperature to probe directly both the development of the ordered Zn and Ta site occupancy within a domain and, separately, the increase in size of these nanoscale domains, under conditions that approximate those used in commercial processing. The high resolution and intensity of the incident synchrotron X-ray beam allows us to study the development of these two separate parameters that are critical in many aspects of modern electroceramic processing,[8] allowing an in situ understanding of the effect of processing details on properties.

Experimental Section

Polycrystalline samples of $Ba_3ZnTa_2O_9$ were prepared from stoichiometric starting mixtures of $BaCO_3$ (Solvay), ZnO (Durham Electrox 2500), and Ta_2O_5 (H. C. Starck). The precursors were ball-milled in distilled water for 16 h using magnesia-stabilized zirconia beads. The dried powders were calcined for 4 h at 1200 °C. High-resolution X-ray powder diffraction data were recorded on beamline BM16[9] at the European Synchrotron Radiation Facility (ESRF), Grenoble, France. Calcined BZT was loaded into a platinum capillary of inner diameter 0.52 mm and 0.04 mm wall thickness. A wavelength of 0.3361 Å (36.88 keV) was chosen as a compromise between the need for hard X-rays to minimize absorption effects due to the platinum capillary while avoiding absorption phenomena from the Ba K edge at 0.3311 Å (37.45 keV). An optical furnace comprising three 150-W halogen lamps was used to heat the sample to a target temperature of 1500 °C over a period of 1 h. Once the annealing temperature was achieved, data sets were recorded every 30 min for a period of some 24 h, the typical operational lifetime of the lamps.

The furnace focuses to a 4-mm section along the sample axis, and thus, no direct measurement of the focal-point temperature during the data collection is possible. Power settings for the furnace were calibrated offline prior to the experiment using a thermocouple in place of the sample. However, both the stability and an in situ calibration of the furnace temperature was afforded by monitoring the unit cell volume of the platinum capillary and comparing values with in situ neutron powder diffraction values. These measurements indicate an operating temperature of some 1200 °C for the experiment and revealed also a linear fall in temperature of some 50 °C during the 24 h experiment due to ageing of the lamps. A second experiment, carried out under the same conditions albeit for a shorter (8 h) period, showed the data to be reproducible, indicating that any changes in the temperature during the runs due to element ageing are not affecting the conclusions drawn. HRTEM measurements were performed on both the starting material and the material recovered from the hot zone of the Pt capillary after the completion of the in situ X-ray diffraction experiments.

Results

Calcined BZT powder was loaded into a platinum capillary, and powder diffraction data were collected on the high-resolution BM16 powder diffractometer at the European Synchrotron Radiation Facility, with the sample temperature (determined as 1200 ± 50 °C) maintained by an optical mirror furnace. Although this annealing temperature is lower than the ∼1500 °C commercially applied for BZT processing, the experiment allows the evolution of cation order and domain size from the pseudocubic disordered starting material to be observed in situ and should allow for the identification of the development of property-critical features of the system during the ordering process.

Data Analysis. The development of long-range order of the Zn and Ta cations on the octahedral B sites of the perovskite structure is signaled by the trigonal distortion of the cubic perovskite subcell and the development of superstructure reflections [such as the (100) used in this experiment]. The supercell reflection intensity can approximately (ignoring incomplete site occupancy and differential Debye−Waller factor effects) be equated with the extent of B site ordering, while the reflection width indicates the spatial extent of the domains within which cation ordering is not interrupted by translational or orientational faults. The evolution of the (100) superlattice reflection intensity with time is shown in Figure 2a.

The (100) superlattice reflection was fitted using a single Lorentzian function. To provide adequate statisti-

(8) Harmer, M. P.; Chen, J.; Peng, P.; Chan, H. M.; Smyth, D. M. *Ferroelectrics* **1989**, *97*, 263−274.

(9) Fitch, A. N. *Mater. Sci. Forum* **1996**, *228*−*231*, 219−222.

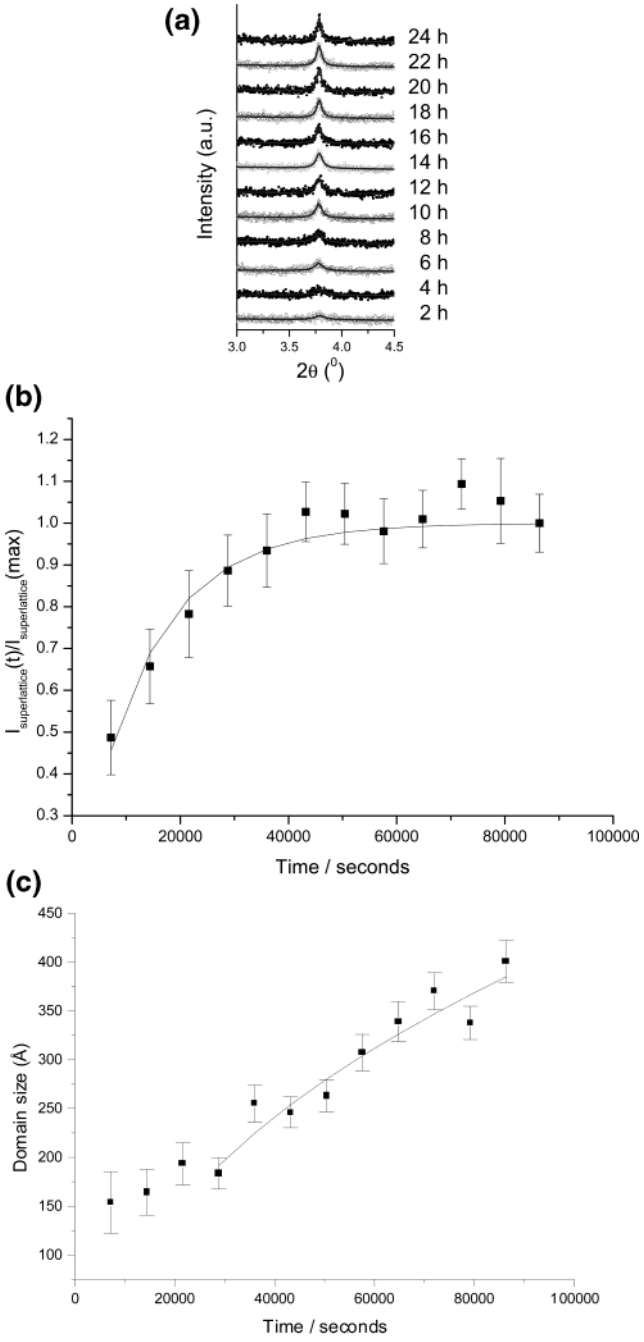

Figure 2. (a) Evolution of the (100) superstructure reflection with the annealing time of BZT. The solid lines are fits to Lorentzian functions that give the intensity and domain size (from the integral breadth) information. (b) Time dependence of the (100) superstructure intensity, *I*, due to ordering of Zn and Ta cations over the octahedral sites. The solid line is a fit to the Avrami−Erofeyev equation with the parameters discussed in the text. (c) Time dependence of the ordered cation domain size, *D*, in BZT during the in situ diffraction experiment. The solid line is a fit to the Allen−Cahn model discussed in the text.

cal quality of the data, in particular during the early stages of annealing, the data sets were summed into 2-h time slices. Figure 2 shows the variation of both (b) the intensity of the (100) superlattice reflection, *I*, and (c) the ordered domain size, *D*, derived from its width with time after the 1200 °C anneal is commenced. This requires the assumption that particle size rather than strain is broadening this reflection.

Full-profile analysis of the data using the Rietveld method reveals a complex phase assemblage, as identified in recent ambient-temperature studies.[10] The high-resolution X-ray powder diffraction data collected during the kinetic runs here require analysis using two similar but distinct BZT phases for all but the earliest stages of annealing. Data for the calcined starting material can be fitted to both a cubic or single trigonal BZT phase [the *c*/*a* ratio of 1.223(1) when the material is refined as trigonal does not differ significantly from the ideal cubic value of $\sqrt{3/2} = 1.224\,745$]. This is consistent with HRTEM observations of some small ordered domains in a largely disordered material (Figure S1, Supporting Information). The size of these ordered domains in the starting material is <10 nm, whereas those in the annealed material measured after the completion of the in situ diffraction measurements are 20−30 nm and extend throughout the sample, in contrast to the starting material (Figure S2, Supporting Information). The calcined starting material is therefore best described as *pseudocubic* and largely B-site disordered. After 2 h of annealing, the data are well fitted to a single *trigonal* BZT phase (Figure 3). Refined parameters indicate only a low-level site ordering of the Zn and Ta cations at this stage. After 6 h of annealing, the single-phase model no longer gives a satisfactory fit to the data, and after 8 h, the development of a second phase is clearly evident. The second phase is seen to evolve with annealing time, and therefore, the two-phase model is best defined in terms of the data set collected after 24 h of annealing (Figure 3). These data are well fitted by a model comprising the initial partially ordered (P) BZT phase, which has sharper diffraction peaks than the second (O) BZT phase that is seen to evolve with annealing time. This second phase is assumed to be fully ordered to make the data analysis tractable, but it will become clear that this assumption, together with the assumption that P is invariant, is an oversimplification. This two-phase model was subsequently refined for all of the kinetics runs, yielding the evolution of the phase fraction, unit cell parameters, and peak widths for the P and O BZT phases. Parameter correlation and the insufficient statistical quality of the data, particularly for the ordered phase in the early stages of annealing, prevented refinement of the degree of cation ordering within each phase with time. No reliable assessment of Zn loss could be made on the basis of the current data.

Discussion

The biphasic nature of the ordered BZT material presents complexity in developing a comprehensive model for the transformation: both phases are at least partially ordered, as they are trigonal, but precise refinement of the extent of order within each phase as a function of time will require data of higher statistical quality. It should be appreciated at the outset of this discussion that both the extent of order and the Zn concentration in the two phases could change with time in a manner to which the current data would be insensitive.

(10) Bieringer, M.; Moussa, S. M.; Noailles, L. D.; Burrows, A.; Kiely, C. J.; Rosseinsky, M. J.; Ibberson, R. M. *Chem. Mater.* **2003**, *15*, 586−597.

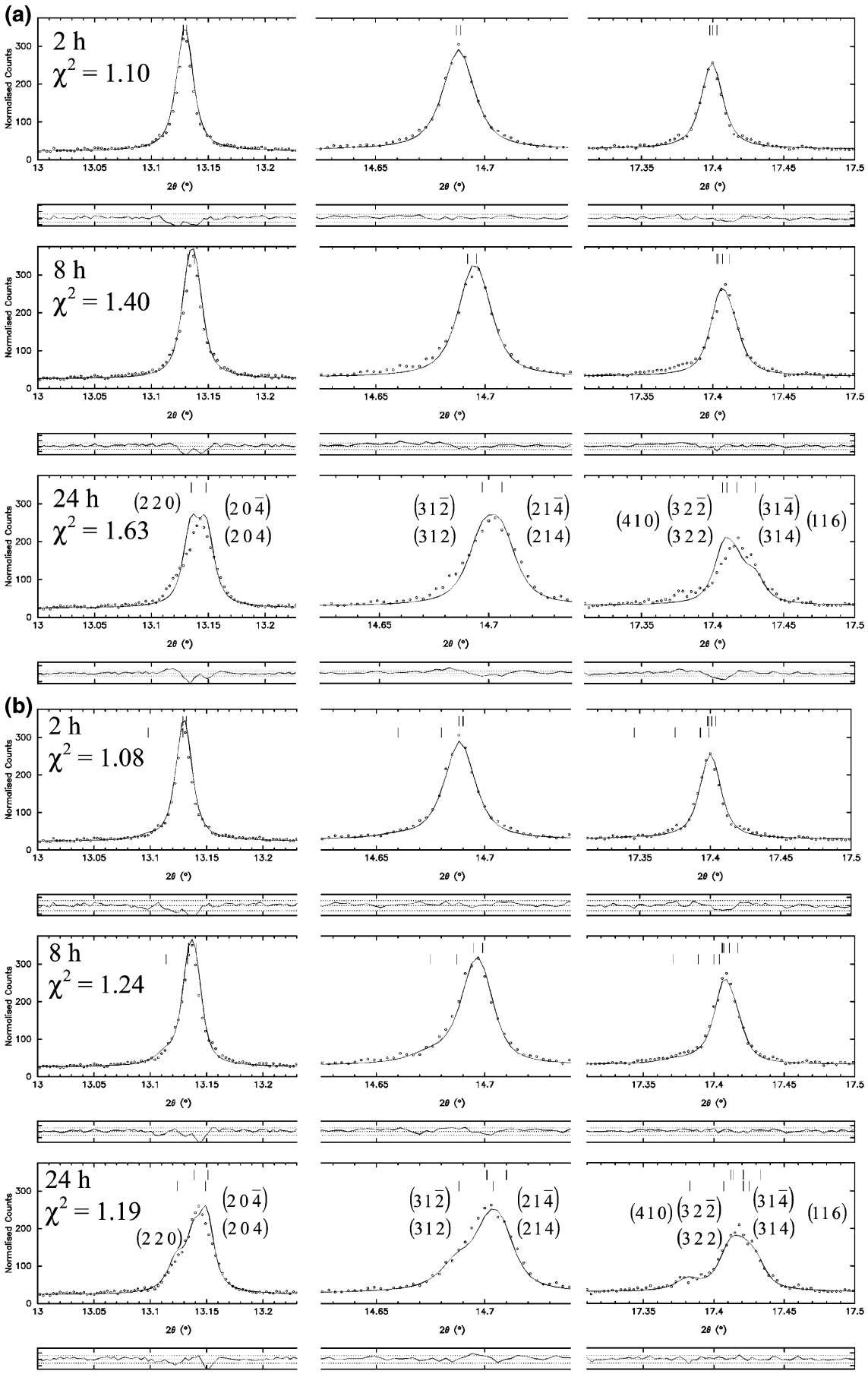

Figure 3. Rietveld analysis of the in situ X-ray powder diffraction data from BZT proceeds satisfactorily with single-phase cubic (0 h) or trigonal (<4 h) models but requires two phases at longer times as the comparison between (a) single- and (b) two-phase fits shows here. The Miller indices of the reflections contributing to the powder profiles in these regions are shown.

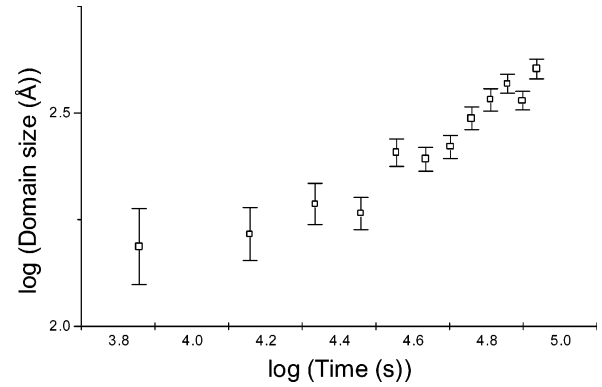

Figure 4. log−log plot of the evolution of the domain size $D(t)$ determined from the (100) superstructure reflection during the annealing of BZT to form the cation-ordered trigonal phase.

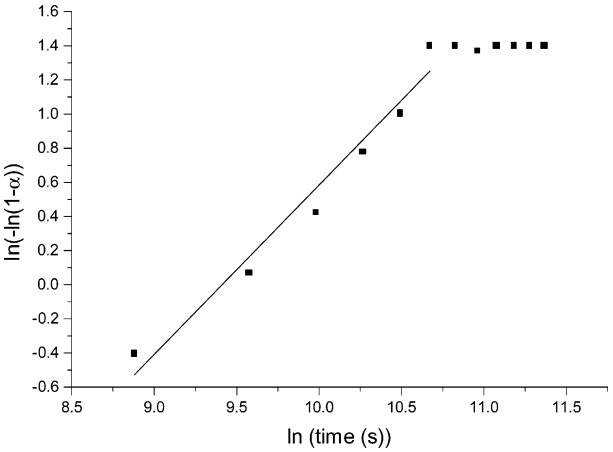

Figure 5. Sharp−Hancock plot of the evolution of the (100) superstructure reflection intensity with time during the annealing of BZT to form the cation-ordered trigonal phase.

The log−log plot in Figure 4 of the evolution of the domain size $D(t)$, determined from the (100) superstructure reflection, shows clearly that there are two qualitatively distinct regions of time dependence. At early times, during the first 8 h of processing, the domain size is effectively constant [with power-law exponent n = 0.14(6)]. At longer times, the domain growth mechanism changes markedly, with an exponent of 0.65(9) indicating more rapid growth.

The evolution of the (100) superstructure intensity $I(t)$ is also complex (Figure 5). It increases rapidly at early times and then becomes effectively constant beyond 8 h, the time at which the superstructure intensity saturates. The variation of the superstructure intensity with time can be quantitatively fitted with the Avrami equation

$$I/I_\infty = \alpha = 1 - \exp(-kt^n) \qquad (1)$$

with n = 0.96(22) and k = 0.000 12(26) s^{-1}.

The Sharp−Hancock analysis, normally used to identify the correct Avrami exponent in the region before completion of the reaction

$$\ln\{-[\ln(1-\alpha)]\} = n \ln t + n \ln k \qquad (2)$$

(Figure 5)[11] indicates a value of n = 1.00(9) and k = 7.5 × 10^{-5} s^{-1}. Final analysis of the intensity data was therefore made using eq 1 with n = 1, which affords k = 8.0(6) × 10^{-5} s^{-1} (Figure 2b). Attempts to fit the higher exponents, n = 3 or 4, expected for three-dimensional nucleation and growth models fail unless unphysical induction periods on the order of the experimental duration are used.

The Avrami model (eq 1) applies to solid-state transformations in which the product phase is nucleated by a fluctuation involving a strong atomic rearrangement on a local scale.[12] The nucleation process has an activation energy due to the interface energy with the untransformed matrix. The growth rate can, in general, be time-dependent and controlled by either interface mobility or bulk diffusion processes: because of the absence of compositional change in order−disorder processes of the type considered here, mass transport within the product phase is usually less important than phase-boundary motion. It should be emphasized that the Avrami treatment of the superstructure data is strictly valid only in the limit of a totally disordered phase transforming into a totally ordered one, as enhanced order within a partially ordered domain will also produce increased superstructure intensities without modifying the volume fraction of the distinct phases. The precise interpretation of the exponent in eq 1 is complex, as the nucleation rate might be constant, increasing, or decreasing during the reaction and the dimensionality of the process also plays a role. In general, $n = \lambda + \beta$, where λ is the dimensionality of the growth and β represents the contribution of the nucleation process and varies between 0 and 1 (0 for instantaneous nucleation, 1 for slow nucleation). The observed exponent in the case of the BZT cation-ordering transformation is consistent with nucleation being unimportant in controlling the transformation kinetics. The n = 1 exponent indicates either site saturation or a one-dimensional growth mechanism in a two-phase order−disorder system. The growth of the order parameter (i.e., the X-ray length-scale-averaged Zn/Ta alternation along the trigonal c axis) is complete after 8 h (Figure 2b), defining the first stage of the transformation. It is important to note that antiphase domain formation does not alter the integrated intensity of superstructure reflections in order−disorder transitions.

In the time region in which the order parameter, as measured by the superstructure intensity, is increasing, the domain size remains constant within error (Figures 2c and 4). This can be understood if nuclei of the ordered trigonal phase are formed within the pseudocubic precursor during the calcination and ramp-to-anneal-temperature stages, and if there is no significant increase in the number of nuclei during the in situ observation period; this is known as "site saturation" in the theory of phase transformations in alloys and is consistent with the growth exponent discussed above. The ordering process as probed by X-rays requires the development of Zn/Ta alternation along the trigonal c axis coherently within a domain. These domains arise from the critical nuclei, which might have the largest value of the Zn/Ta short-range order parameters in the

(11) Sharp, J. H.; Hancock, J. D. *J. Am. Ceram. Soc.* **1972**, *55*, 74−77.

(12) Christian, J. W. *The Theory of Transformations in Metals and Alloys*; Pergamon Press: Oxford, U.K., 1975.

precursor, at a critical size as soon as the annealing procedure begins. They do not grow in extent further during the initial 8 h stage. This initial stage then corresponds to the development of long-range order *within* the domains. The observed kinetics would be consistent with the Zn/Ta interchanges occurring within a domain in one dimension (the *c* axis within that domain) to produce the required trigonal layered structure of Figure 1b, although the caveats concerning the strict applicability of the Avrami equation to this case should be kept in mind. This first stage ends when the domains impinge on each other and the ordering integrated over all of the domains in the sample has reached its maximum value accessible at the annealing temperature. This is important, as the high resolution of our data shows that the material is actually biphasic at this stage (Figure 3). The second stage of the transformation involves the conversion of phase P into phase O without the extent of order *as quantified by the superstructure intensity* changing. The growth in the initial period does not involve the formation of larger domains but the continuous development of order within them until the ordered (O) and partially ordered (P) phases impinge on each other. The observed value of $n = 1$ is a strong indicator that the formation of nuclei does not play a role in the observed kinetics — the nuclei are preformed by the previous stages of the thermal treatment.

Once the order within the domains is completed, individual domains differ in either the orientation or phase of the order parameter, producing high-energy domain boundaries. The late stages of many ordering transitions in alloys are characterized by a domain coarsening transition in which the domain size *D* increases as driven by the minimization of the curvature at the interface between neighboring domains.[13] This gives a $D \sim t^{1/2}$ scaling relationship according to the Lifshitz−Allen−Cahn model,[14] which is obeyed within error by our data in the period beyond 8 h (Figure 2c).

There are, in principle, three distinct transformation mechanisms in solids: heterogeneous, homogeneous, and spinodal.[15] The observation of distinct BZT phases here, formed from a single-phase pseudocubic calcined precursor, indicates that heterogeneity develops during the ordering transition. This is clearly consistent with a nucleation and growth model in which the ordered phase grows from a disordered matrix and indicates that the single-exponential superlattice reflection intensity evolution is not solely due to spinodal or continuous homogeneous ordering. This is an oversimplification of the situation in BZT domain growth, however, as *both* phases are trigonal and, therefore, at least partly ordered at all stages of the transition, posing a difficulty for application of the Avrami treatment of the superstructure intensities. The weakness of the superstructure reflections and the similarity of the atomic positions in the two phases restrict the level of discrimination between the two phases in the Rietveld analyses, but the evolution of the two phases during the annealing procedure is clear. Phase 1 (P) is the majority phase at the start of the transformation and has a *c*/*a* value distinct from that of phase 2 (O), which grows in upon annealing. Phase O refines to have essentially complete Zn/Ta ordering and, consistent with its *c*/*a* value, differs more strongly from the pseudocubic values than P. However, we cannot rule out the possibility that the extent of order and other key structural parameters such as the Zn concentration vary in *both* phases during the second stage of the transformation. The evolution of the phase fractions of these two phases, both with Zn/Ta ordering, during the high-temperature treatment, indicates that the formation of a single ordered BZT phase is considerably more complex than the observation of saturation of the superstructure intensity alone would suggest. There is a significant redistribution of the Bragg intensity between the subcell reflections of the two phases at times considerably longer than the 8 h required to saturate the integrated intensity of the superstructure reflections.

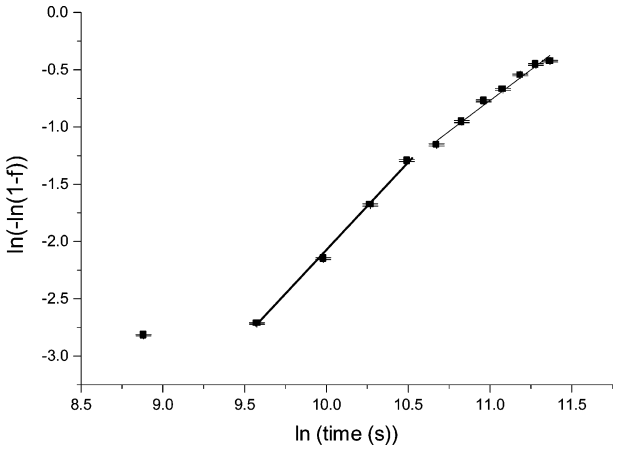

Figure 6. Sharp−Hancock plot of the variation of the fraction *f* of the fully ordered phase O as a function of time shows a crossover from an Avrami exponent in eq 1 of $n = 1.07(6)$ for the first 10 h of the annealing process to $n = 1.55(5)$ for the remaining time.

A Sharp−Hancock plot of the variation of the fraction of phase O with time (Figure 6) reveals a mechanistic crossover in the evolution of the phase fractions *at the same time as the overall extent of order* (quantified by the superstructure intensity) *saturates and the domain growth begins*. The second stage of the transformation occurring during annealing corresponds to changing of the phase fractions of the O and P phases and appears to be coupled with the onset of domain growth. This confirms the mechanistic change apparent from the analysis of the superstructure intensities and is consistent with domain growth being driven by the increased phase fraction of the O phase. It is important to note that the total superstructure intensity is saturated during this part of the transformation, so a conventional order−disorder interpretation in terms of P transforming into fully ordered O is not possible: O and P must differ to a greater degree than the extent of order within them. The role of the B-site Zn concentration in this phenomenon should be the focus of further studies. The *c*/*a* value (Figure 7) of the O phase remains constant within error during the annealing period, whereas that of P changes, suggesting a change in this phase during the annealing, consistent with the idea that this phase is not simply fully disordered O that remains constant throughout the transformation. The

(13) Nagler, S. E.; Shannon, R. F., Jr.; Harkless, C. R.; Singh, M. A.; Nicklow, R. M. *Phys. Rev. Lett.* **1988**, *61*, 718−721.
(14) Allen, S. M.; Cahn, J. W. *Acta Metall.* **1979**, *27*, 1085−1095.
(15) Irani, R. S. *Contemp. Phys.* **1972**, *13*, 559−583.

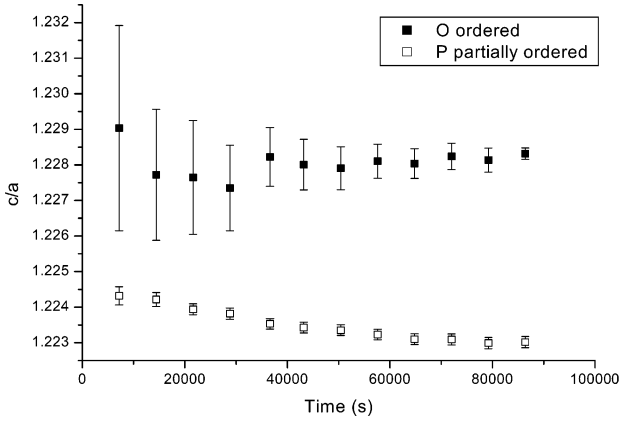

Figure 7. Time evolution of the *c*/*a* ratio of the two BZT phases required for full-profile analysis of the diffraction patterns. Figures S3 and S4 (Supporting Information) show polynomial fits to these data, demonstrating that the change in the *c*/*a* value of phase P is statistically significant.

domain growth observed in the second stage of the transformation is driven by loss of phase P and growth of phase O, and the atomic motions involved in the two processes might well be coupled. The evolution of the order within the domains at constant size (stage one of the ordering process) is reflected here by the evolution in the *c*/*a* ratio of the partially ordered phase and the growth in the phase fraction of the ordered phase.

The nucleation might take place in the 0−2 h period, or the precalcination treatment, and it might occur in regions of the sample that have the largest amount of short-range order; further experiments with better time resolution and signal-to-noise ratio are required to investigate this issue. The observation of two distinct phases means that the exponential growth of the superstructure intensity contains information about the nucleation and growth of ordered BZT within the partially ordered matrix.

Conclusions

These time-resolved X-ray data allow us to understand the origin of the time dependence of the key parameter, *Q*, in the processing of BZT. At early stages (0−8 h), ordering occurs within domains of constant size, nucleated presumably within regions of maximal Zn/Ta short-range order in the precursor prepared in the initial thermal treatment. If this process is intrinsically related to the kinetics of interchange of Zn and Ta on the octahedral sites of the perovskite structure, then all BZT-related phases, independent of the identity of the B-site dopant, will need anneals at least on the order of hours to maximize *Q* (e.g., 24 h used in commercial Zr or Ga B-site doped materials), because maximizing this order within even nanoscale domains is a prerequisite for high *Q*.

The later stages of the process involve domain growth, which proceeds with a power-law mechanism characteristic of curvature-induced domain coarsening. The influence of this step on *Q* will depend on how deleterious an effect the domain walls have on *Q*; if they are severely degrading (as in BZT itself[6]), then large domains are needed, and extremely long annealing times will be required. If the domain walls are not detrimental, then only the intradomain ordering is required for high *Q*, and although annealing can increase the domain size, it will have only a minor effect on *Q*.

The B-site cation order develops with time when monitored simply by the superstructure reflection intensity, as predicted by a simple Avrami model, but the Rietveld refinement of the whole pattern shows that this extent of order is actually distributed between two phases with distinct *c*/*a* ratios. The phase coexistence is not a consequence of the simple coexistence of ordered and disordered phases in a nucleation and growth model, followed by coarsening of the domains, because both phases are trigonal and thus at least partially ordered. The ordering saturates before domain growth couples with the transformation of phase P into phase O.

This in situ study is currently at the technical limits of what can be achieved on an electroceramic system. Nevertheless, it has identified the complex issues of phase separation during annealing and ordering (which might be related to Zn loss) and the existence of two different kinetic regimes in the annealing process. Both need to be explained before a comprehensive understanding of the factors controlling BZT processing can be claimed. The high resolution of the X-ray data is key in observing both the domain size variation and the phase separation during annealing. Many electroceramic properties depend on both order and the spatial extent of the order, and this study demonstrates that these properties can be probed independently in situ during materials processing as a function of time over length scales down to the nanoscale. Understanding the origin of the features revealed by combining the high-resolution diffraction data with time resolution compatible with the time scale of the commercial processing at high temperature will improve our ability to process such complex oxide materials.

Acknowledgment. We thank Professor C. J. Kiely and Dr. A. Burrows (Materials Science Division, Department of Engineering, University of Liverpool) for the HRTEM measurements. We thank D. Iddles (Filtronic Comtek) and I. M. Reaney (University of Sheffield) for useful discussions. We thank the U.K. EPSRC for support under GR/M62433.

Supporting Information Available: HRTEM images of the starting material and the material after heating in the X-ray beam. Polynomial fits demonstrating that *c*/*a* is unchanged within error for phase O but changes with time in a statistically significant manner for phase P. This material is available free of charge via the Internet at http://pubs.acs.org.

CM020476C